

Supplemental information

**Protective role for kidney *TREM2*^{high} macrophages
in obesity- and diabetes-induced kidney injury**

Ayshwarya Subramanian, Katherine A. Vernon, Yiming Zhou, Jamie L. Marshall, Maria Alimova, Carlos Arevalo, Fan Zhang, Michal Slyper, Julia Waldman, Monica S. Montesinos, Danielle Dionne, Lan T. Nguyen, Michael S. Cuoco, Dan Dubinsky, Jason Purnell, Keith Keller, Samuel H. Sturner, Elizabeth Grinkevich, Ayan Ghoshal, Amanda Kotek, Giorgio Trivioli, Nathan Richoz, Mary B. Humphrey, Isabella G. Darby, Sarah J. Miller, Yingping Xu, Astrid Weins, Alexandra Chloe-Villani, Steven L. Chang, Matthias Kretzler, Orit Rosenblatt-Rosen, Jillian L. Shaw, Kurt A. Zimmerman, Menna R. Clatworthy, Aviv Regev, and Anna Greka

Supplementary Figure Legends

Supplementary Figure 1. Phenotypic characterization of mouse DKD models

(A) Assessment of podocytes in glomeruli from patients with and without DKD using *in situ* HCR with probes complementary to podocin (*NPHS2*; red) and synaptopodin (*SYNPO*; green). *LRP2* (megalyn; cyan) delineates the proximal convoluted tubules (DAPI; blue); scale bar 50 μ m. Podocytes were quantified in three independent fields of view for each of the DKD and non-DKD samples.

(B) Quantification of podocytes by *in situ* HCR in patients with and without DKD. Mean podocyte percentage: 26.2% \pm 1.74% in non-DKD versus 18.1% \pm 0.27% in DKD, ****p<0.01** (unpaired Student's t-test).

(C) Phenotypic characterization of the HFD-fed mice including serum creatinine concentration and albuminuria quantification, ***p<0.05**, ****p<0.01**, *****p<0.001**. Serum creatinine chow (n = 32), HFD (n = 37), p<0.0001; urine albumin for chow (n = 57) and HFD (n = 106).

(D) Light and transmission electron microscopic examination of kidney tissue from chow and HFD-fed mice.

(C-L) Metabolic profile of chow- and HFD-fed mice: body weight (E), glucose tolerance test (F), insulin tolerance test (G), and plasma levels of insulin (H), adiponectin (I) and leptin (J). Body fat percentage (K, plasma cholesterol level (L), triglyceride level (M) and bone mineral density (N) are also shown. Chow (n = 33); HFD (n = 39); Mean \pm S.E.M. ***p<0.05**, *****p<0.001**.

(M-N) Glucose (O) and insulin (P) tolerance tests in 5- and 10-week-old BTBR *wt/wt* and *ob/ob* mice, respectively. BTBR *wt/wt* 5wk n= 9; *ob/ob* 5wk n = 9; BTBR *wt/wt* 10wk n= 9; *ob/ob* 10wk n = 9; Mean \pm S.E.M.

(O-Q) Measurement of renal parameters in 5- and 10-week-old BTBR *ob/ob* mice; 24h urinary albumin (Q), blood urea nitrogen (BUN, R)) and serum creatinine (S). Mean \pm S.E.M. *****p<0.001**

(T) Plasma total cholesterol levels in 5- and 10-week-old BTBR mice. Mean \pm S.E.M. *****p<0.001**.

(L) Transmission electron microscopy of kidney tissue from 10-week-old BTBR *wt/wt* and *ob/ob* mice.

Supplementary Figure 2. DKD in mouse and human kidney tissue at single cell resolution

(A, B) UMAP plots of the cell populations identified in nephrectomy specimens from patients (A) with DKD (N=3) and (B) without DKD (N=9). Individual populations are represented by distinct colors.

(C, D) UMAP plots of cells recovered from the kidneys of (C) HFD- and (D) chow-fed mice (N=4 in each condition). Individual populations are represented by distinct colors.

(E, F) UMAP plots of cell populations identified in the kidneys of 5-week-old BTBR (E) *ob/ob* and BTBR (F) *wt/wt* mice. (N=5 in each condition) Individual populations are represented by distinct colors.

(G, H) UMAP plots of cell populations identified in the kidneys of 10-week-old BTBR (G) *ob/ob* and BTBR (H) *wt/wt* mice (N=3 in each condition). Individual populations are represented by distinct colors.

(I-L) Number of differentially expressed genes (FDR < 5%) by cell class for the mouse models (Wilcoxon-rank-sum test): human data (I, Poisson mixed-effects model, FDR<0.1), HFD (J), BTBR 5wk (K), and BTBR 10wk (L).

(M-P) UpSet plots representing shared and unique signatures among the human and mouse DKD data in the (M) DCT, (N) TAL, (O) podocyte and (P) mesangial cells. The set size represents the total number of differentially expressed genes in DKD. The intersection size represents the number of genes in the intersection of the sets represented by the black dots connected by the line segment. In podocytes and mesangial cells, the transcriptional response to disease varied between mouse and human, both in terms of the specific genes affected and the direction of the effect.

Supplementary Figure 3. Changes in podocyte, mesangial and Proximal Convoluted Tubular (PCT) cell DKD-related gene expression

(A) Boxplots showing normalized gene expression of *Col4a3* in podocytes from mouse models. From left to right: BTBR *wt/wt*, and BTBR *ob/ob* 5 wk, 10wk, and chow-fed, HFD mouse models.

(B) Representative *in situ* HCR images and quantification of *Col4a3* expression in podocytes of 10-week-old BTBR *wt/wt* (mean 0.24 \pm SEM 0.02; n=3) and BTBR *ob/ob* (mean 0.46 \pm SEM 0.02; n=3) mice. Scale bars 50 μ m. ****p < 0.01**, unpaired Student's t-test.

(C) Boxplots showing normalized gene expression of *Col4a2* in mesangial cells from DKD mouse models. From left to right: BTBR *wt/wt*, and BTBR *ob/ob* 5 wk, 10wk, and chow-fed, HFD mouse models.

(D) Representative *in situ* HCR images and quantification of *Col4a2* in mesangial cells of 10-week-old BTBR *wt/wt* (mean 0.72 +/- SEM 0.02; n=5) and *ob/ob* (mean 1.77 +/- SEM 0.09; n=5) mice. Scale bars 50 μ m. ***p < 0.001, unpaired Student's t-test.

(E-G) Boxplots showing normalized gene expression of *Pck1* (E), *Lrp2*(F), *Gsta2*(G) in proximal convoluted tubule cells from DKD mouse models. From left to right: BTBR *wt/wt*, and BTBR *ob/ob* 5 wk, 10wk, and chow-fed, HFD mouse models.

(H) (left) Immunofluorescent staining of *Pck1* (red) in kidney tissue from chow- and HFD-fed mice. (right) Quantification of *Pck1* immunofluorescence in kidneys from chow- (mean 7.28 +/- SEM 0.25; n = 5) and HFD-fed mice (mean 10.06 +/- SEM 1.09; n = 5); ** p<0.01, FU, fluorescence units. Scale bars 50 μ m.

(I) (left) *In situ* HCR for expression of *Lrp2* (green), *Pck1* (red), *Gsta1/2* (cyan) in kidneys from 10-week-old BTBR *wt/wt* and BTBR *ob/ob* mice.

(middle) Quantification of *Pck1* expression in 10-week-old BTBR *wt/wt* (n=4) and BTBR *ob/ob* (n=4) mice by *in situ* HCR; *p<0.05, unpaired Student's t-test. RFU, relative fluorescence units.

(right) Quantification of *Gsta1/2* expression in 10-week-old BTBR *wt/wt* mice (mean 1.82 +/- SEM 0.08; n=4) and BTBR *ob/ob* mice (mean 12.37 +/- SEM 1.75; n=4) by *in situ* HCR; *** p < .001, unpaired Student's t-test. RFU, relative fluorescent units.

Supplementary Figure 4. Macrophage cell populations present in the kidneys of the HFD and BTBR mice and validation in the UK cohort

(A) UMAP visualization of resident M Φ pan-marker and subset specific marker genes in the kidney meta-atlas.

(B) Dot plot visualization of marker genes (columns) from *LYVE1* macrophages in the heart (PMID: 32971526) distinguishing myeloid subsets (rows). Size of the dots represent the proportion of cells in each subset (columns) expressing the gene (rows). Color of the dots represents the normalized average expression in units of log(TPX+1).

(C) UMAP visualization of myeloid cells in the KPMP scRNA-seq dataset (N=45).

(D) Heatmap visualization of cluster specific marker genes. Cluster 5 was enriched for the *TREM2* program.

(E) UMAP visualization of *TREM2*^{high} macrophages in healthy donors and patients with hypertensive chronic kidney disease (H-CKD) or diabetic kidney disease (DKD)

(F) Heatmap showing DE genes characterizing kidney resident and infiltrating macrophage populations in the two mouse models (HFD and BTBR) and time points (5- and 10-week-old BTBR).

(G) UMAP plots of M Φ cell populations identified in the kidneys of 5-week-old BTBR *wt/wt* and BTBR *ob/ob* mice. Individual populations are represented by distinct colors.

(H) Heatmap showing canonical and data-derived DE genes used for immune cell cluster annotation in chow- and HFD-fed mice.

(I) Heatmap showing canonical and data-derived DE genes used for 5-week-old BTBR *wt/wt* and BTBR *ob/ob* mouse kidney immune cell cluster annotation.

(J) Heatmap showing canonical and data-derived DE genes used for immune cell cluster annotation in 10-week-old BTBR *wt/wt* and BTBR *ob/ob* mice.

(K) Comparison of macrophage populations between mouse strains to show shared and unique populations. Comparisons were performed by training a classifier on the HFD model macrophages and predicting labels on the 5-week-old BTBR macrophage data.

(L) Correlation between BMI (20-60) and *TREM2*⁺ macrophages % of CD163⁺ cells/ROI with the outlier included. ROI; region of interest. R = 0.34; p = 0.02.

(M) Correlation between BMI (20-60) and *TREM2*⁺ macrophages % of CD163⁺ cells/ROI with the outlier excluded. ROI; region of interest. R = 0.32; p = 0.03.

(N) Dotpot visualization of *Trem2* expression among all kidney cell types in the HFD model of DKD. The size of the dots represents the proportion of cell in the cell type (rows, Y-axis) that express the gene and the color represents average gene expression in units log(TPX+1).

Supplementary Figure 5. HFD-treatment induced podocyte foot process effacement and tubular cell mitochondrial injury in *Trem2*^{-/-} mice.

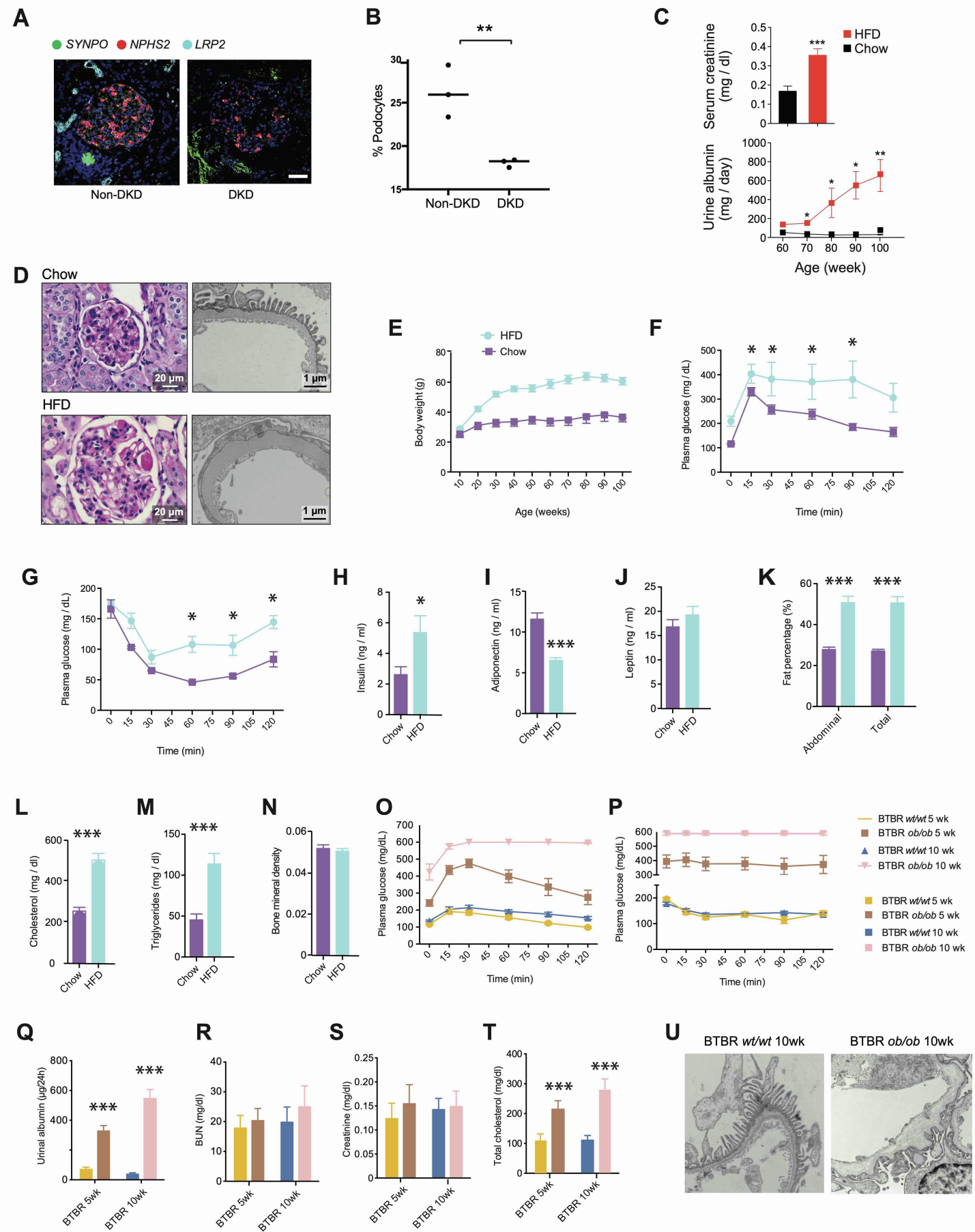
(A) CRISPR-cas9 knockout strategy for *Trem2*^{-/-} mice.

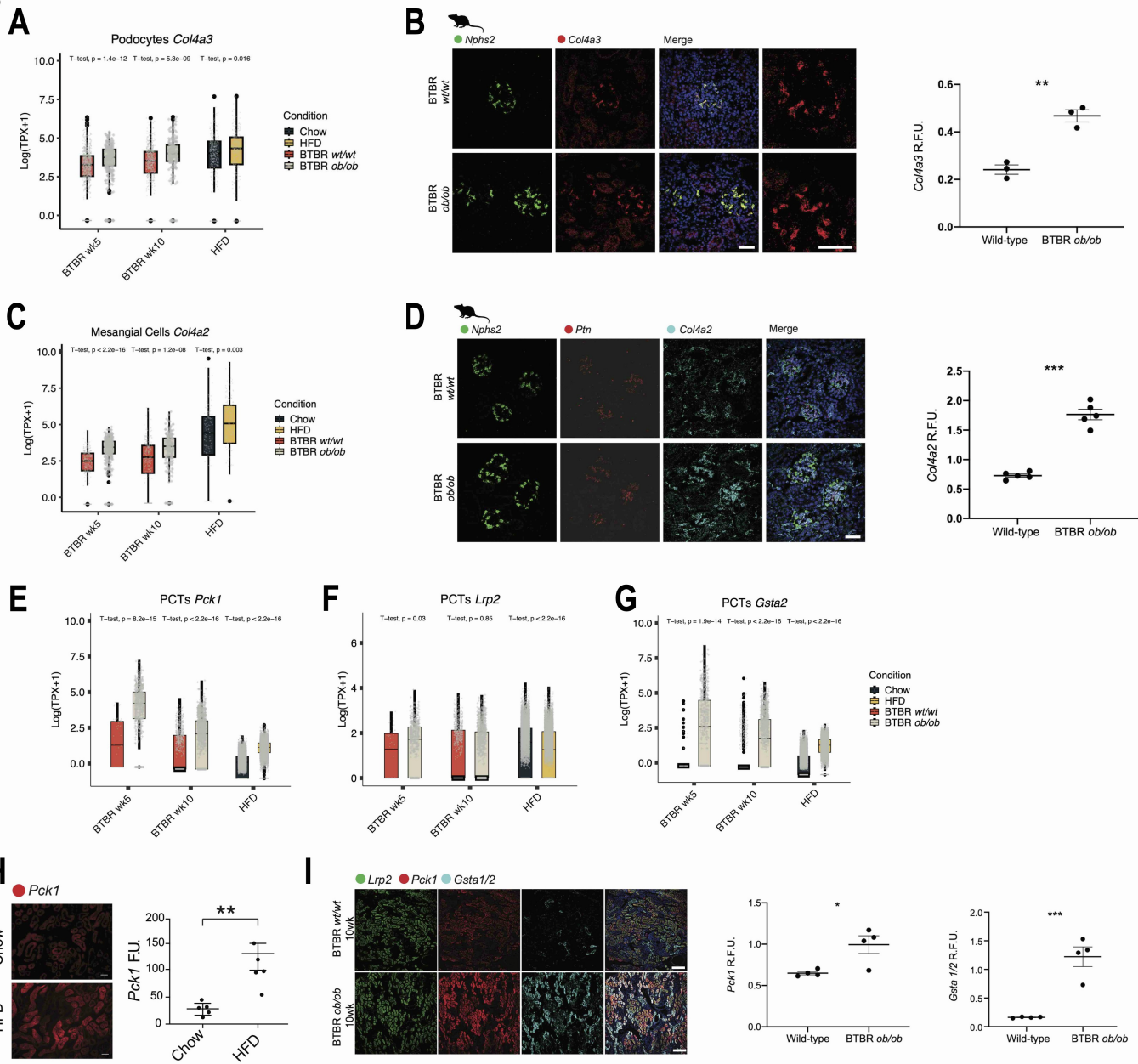
(B) PCR validation of *Trem2* gene in WT and *Trem2*^{-/-} mice. Primer set 1 and 2 for amplification of KO and WT regions, respectively.

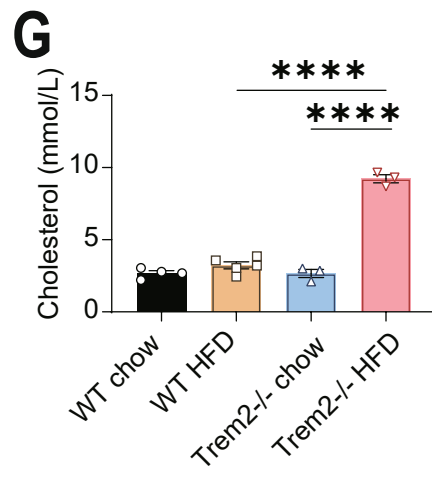
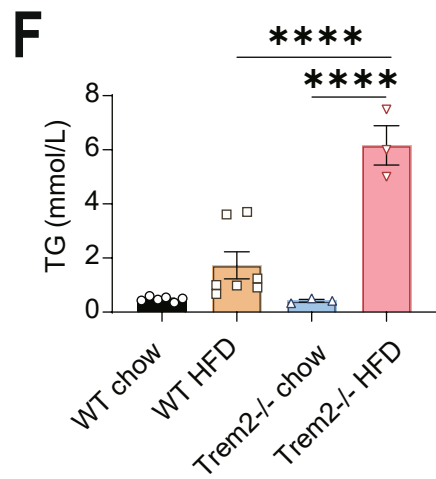
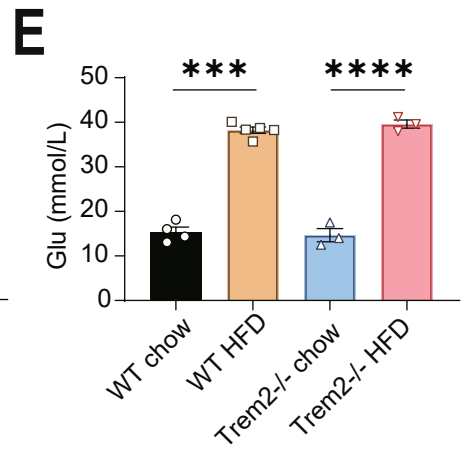
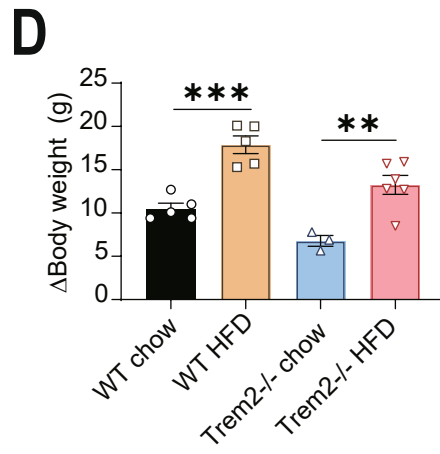
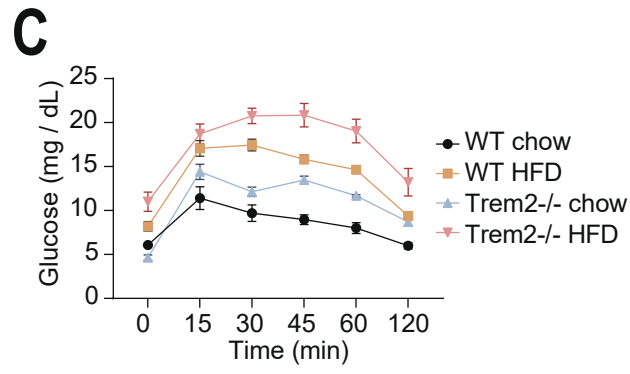
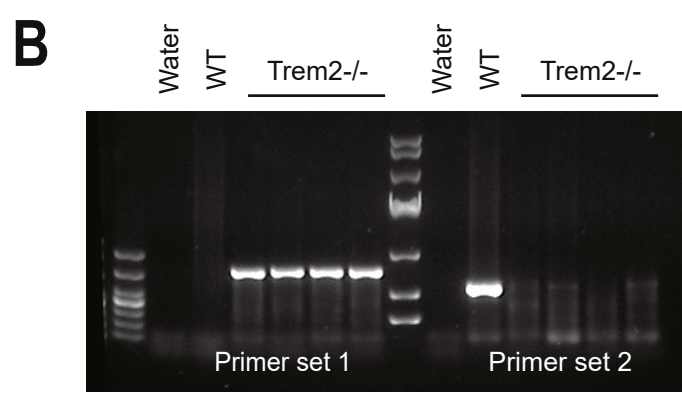
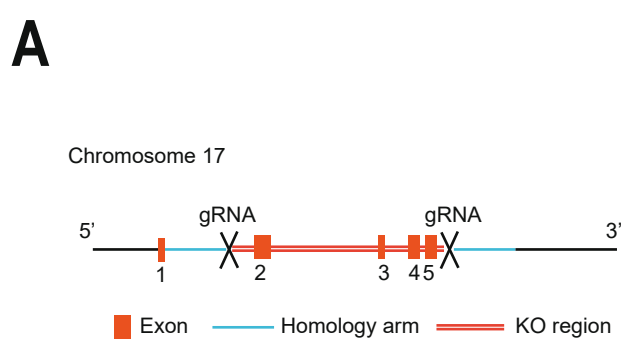
(C) Glucose tolerance test of WT chow, WT HFD, *Trem2*^{-/-} chow, and *Trem2*^{-/-} HFD mice.

(D-G) Histograms of changes in body weight gain (D), serum glucose (E), triacylglycerol (F), and cholesterol levels (G) in WT and *Trem2*^{-/-} HFD mice treated with chow and HFD. **P < 0.01, ***P < 0.001, ****P < 0.0001. Mean ± S.E.M.

S1







Supplementary Table 7 Main demographic and clinical characteristics of kidney donors, relevant to Figures 3H, I

	All N=45	Healthy (A) N=16	HTN (B) N=8	P value A vs B	Obese (C) N=13	P value A vs C	Diabetic (D) N=8	P value A vs D
Male, n (%)	29 (64)	9 (56)	5 (62)	1	9 (69)	0.70	6 (75)	0.65
Age, median (IQR) –years	62 (49-70)	46 (22-63)	67 (61-76)	0.021	61 (58-69)	0.035	69 (58-72)	0.10
Cause of death, n (%)								
Cerebral event	30 (66)	7 (44)	6 (75)	0.21	10 (77)	0.12	7 (87)	0.07
Cardiorespiratory	10 (22)	5 (31)	2 (25)	1	2 (15)	0.41	1 (13)	0.62
Trauma	4 (9)	3 (19)	0	0.53	1 (8)	0.60	0	0.52
Other	1 (2)	1 (6)	0	1	0	1	0	1
sCr at retrieval, median (IQR) – μM/L	72 (59-88)	73 (59-96)	57 (51-70)	0.11	75 (67-85)	0.83	85 (78-97)	0.35
eGFR at retrieval, median (IQR) – mL/min/1.73 m ²	95 (88-111)	94 (78-112)	99 (90-112)	0.58	98 (78-111)	0.88	96 (90-101)	0.95
Arterial hypertension, n (%)	23 (51)	0	8 (100)	<0.001	10 (77)	<0.001	6 (75)	<0.001
Treatment, n (%)								
RAAS inhibitors	12/23 (52)	--	4 (50)	--	4/10 (40)	--	4/6 (66)	--
Calcium channel blockers	7/23 (30)	--	2 (25)	--	3/10 (30)	--	2/6 (33)	--
Other	7/23 (30)	--	3 (37)	--	1/10 (10)	--	3/6 (50)	--
None/diet	6/23 (26)	--	2 (25)	--	4/10 (40)	--	2/6 (33)	--
BMI, median (IQR)	27 (24-32)	25 (23-27)	24 (23-27)	0.83	34 (32-36)	<0.001	32 (28-34)	0.012
BMI ≥30, n (%)	19 (42)	0	0	1	13 (100)	<0.001	6 (75)	<0.001
Diabetes, n (%)	8 (18)	0	0	1	0	1	8 (100)	<0.001
Treatment, n (%)								
Insulin	0	--	--	--	--	--	0	--
Metformin	4/8 (50)	--	--	--	--	--	4 (50)	--
SGLT2i	0	--	--	--	--	--	0	--
Other	1/8 (12)	--	--	--	--	--	1 (12)	--
None/diet	4/8 (50)	--	--	--	--	--	4 (50)	--

BMI, body mass index; HTN, hypertensive; IQR, interquartile range; sCr, serum creatinine

RAAS inhibitors include angiotensine converting enzyme inhibitors and angiotensine II receptor blockers